ChemComm

COMMUNICATION

View Article Online
View Journal | View Issue

Cite this: *Chem. Commun.*, 2016, 52, 11359

Received 7th May 2016,
Accepted 24th August 2016

DOI: 10.1039/c6cc03847f

www.rsc.org/chemcomm

Electron–phonon coupling in engineered magnetic molecules†

Violeta Iancu,*[ab] Koen Schouteden,[a] Zhe Li[a] and Chris Van Haesendonck[a]

We probe the electron–phonon coupling for *in situ* engineered porphyrin-based magnetic molecular layers supported on weakly reactive surfaces. Using high-resolution scanning tunneling microscopy and spectroscopy at 4.5 K we show that the electronic and magnetic properties of the engineered molecules are the result of interplay between many-body spin–flip excitations and electron–phonon interactions.

Metallo-porphyrins are widely found in biological systems (chlorophyll-a, heme) and their functionality is further explored for use in artificial systems.[1] Metallo-porphyrins are easily vapor-deposited and adsorbed on metallic surfaces to mimic and investigate possible working configurations in future molecular devices.[2] Tetrapyridyl pophyrin (5,10,15,20-tetra(4-pyridyl)-21*H*, 23*H*-porphine, TPyP), a porphyrine derivate investigated in this work, has shown great versatility in terms of self-assembly, doping and property tuning.[3–6] For instance on an atomically clean Au(111) surface, TPyP can form a large variety of molecular structures with different packing densities,[5,7,8] whereas on Ag(111) the molecules form only close-packed structures.[3,4,6] The versatility of these molecules extends beyond their 2D assembly capabilities and by a simple magnetic atom doping their properties can be conveniently tailored *ad hoc*.[6,9] Numerous experimental and theoretical studies showed how electrons (from leads and supporting substrates) interacting with molecules can have exciting consequences and reveal interesting phenomena among which Kondo effect,[10–14] negative-differential resistance,[15,16] Coulomb blockade,[17] and vibronic coupling.[18]

Here, we investigate the electronic transport through magnetic TPyP molecules supported by a Au(111) surface and measured with a tungsten scanning tunneling microscope (STM) tip to probe electron–phonon coupling. The magnetic molecules were synthesized *in situ* through chemical reactions between non-metallic porphyrin-based molecules and magnetic (Co, Cr) atoms, an established procedure to create and study exotic molecules in a highly controlled environment.[6,9,19–21] Conductance measurements through molecules at low temperatures reveal pronounced Kondo resonances at zero bias and additional Kondo resonance replicas observed at higher voltages in vibrating CoTPyP molecules. The Kondo resonance replicas are observed only in the presence of electron–phonon interactions and are associated with creation and destruction of phonons.[22] Adatom coverages in excess of one adatom per molecule lead to the formation of highly organized structures of magnetic molecules and metallic clusters.

Fig. 1 presents the TPyP molecules adsorbed on Au(111) after doping with Co (Fig. 1(a)) and Cr (Fig. 1(b)) atoms.[23] The TPyP molecules are non-metallic porphyrin-based systems that consist of a porphyrin macrocycle and four pyridyl groups at the periphery. By doping we mean the substitutional insertion of a single magnetic atom at the center of the porphyrin macrocycle, as is schematically described in Fig. 1(c).[24] The TPyP molecules were vapor-deposited (at 550 K) and adsorbed on a clean Au(111) surface held at room temperature to form close-packed molecular islands (see Section I in ESI† for more details on TPyP self-assembly on Au(111)). Minute amount of either Co or Cr (0.09 monolayer (ML) of Co and 0.05 ML of Cr; 1 ML = 1.38×10^{15} atoms per cm^2) were subsequently deposited onto the close-packed TPyP structures kept at room temperature. Further annealing to 530 K for 60 minutes was used to activate the chemical reactions and to achieve homogeneously doped molecular layers. The successful molecular doping is inferred from visual inspection of the STM images and electronic property measurements of the molecules (discussed later in the article). The appearance of the molecule changes upon doping: the original depression at the center transforms into a protrusion after atom insertion (Fig. 1(c)). Measurements of the molecular apparent height indicate about

[a] *Laboratory of Solid-State Physics and Magnetism, KU Leuven, BE-3001 Leuven, Belgium. E-mail: Violeta.Iancu@eli-np.ro, Chris.VanHaesendonck@fys.kuleuven.be*
[b] *Extreme Light Infrastructure – Nuclear Physics/Horia Hulubei National Institute for R&D in Physics and Nuclear Engineering, Bucharest-Magurele, RO-077125, Romania*

† Electronic supplementary information (ESI) available: (I) TPyP adsorption on Au(111) and the metalation of porous structures; (II) additional scanning tunneling spectroscopy data for CoTPyP networks; (III) STS of metallic intermolecular junctions formed after Cr deposition. See DOI: 10.1039/c6cc03847f

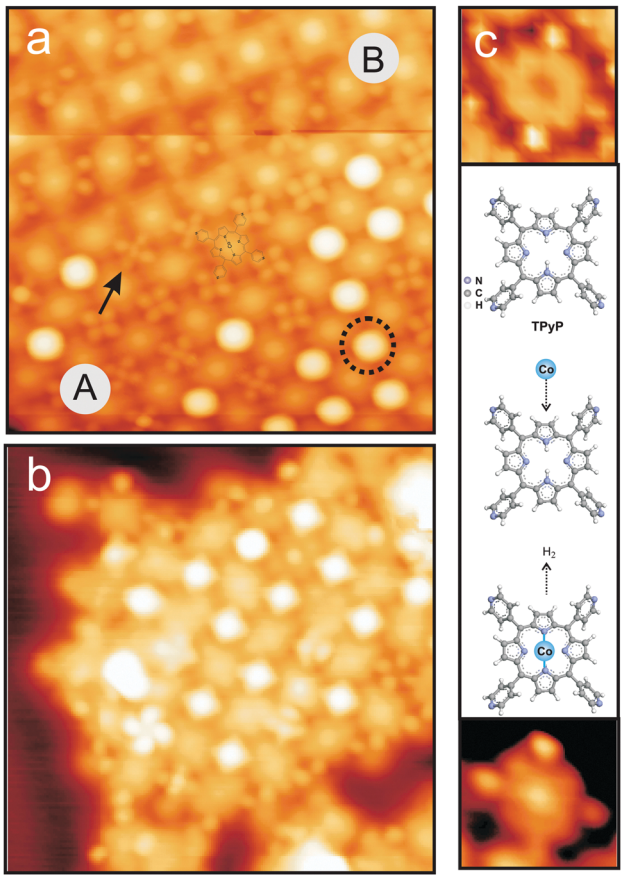

Fig. 1 (a) STM image of the CoTPyP assemblies on Au(111). Image parameters: 10 nm × 10 nm, 50 mV, 50 pA. (b) STM image of the CrTPyP assemblies on Au(111). Image parameters: 10 nm × 10 nm, 500 mV, 100 pA. (c) Schematics describing the formation of magnetic molecules upon N–H bond breaking, metal atom insertion and release of H_2 molecule (illustrated for Co atoms) together with two high resolution STM images showing the TPyP molecule before (top) and after (bottom) Co insertion at the macrocycle. STM images parameters: −1 V, 100 pA.

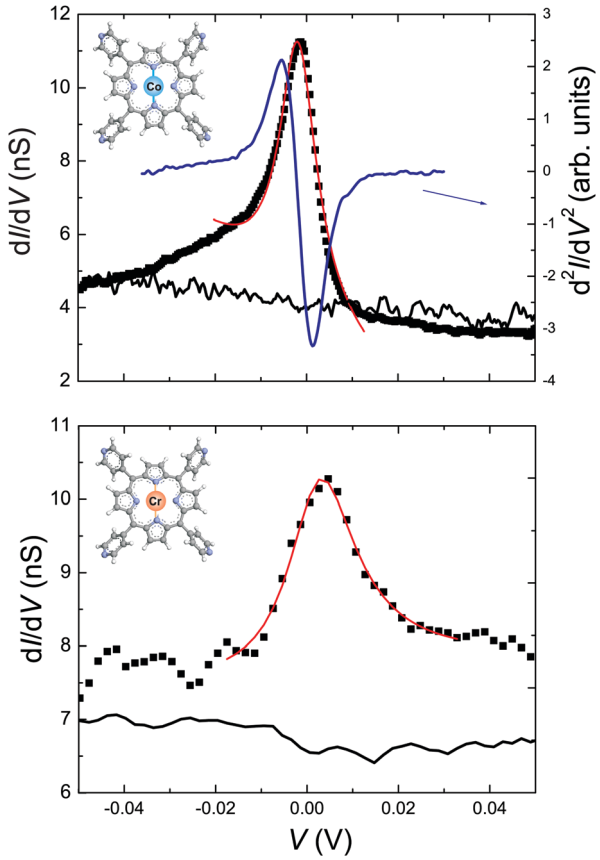

Fig. 2 d*I*/d*V* (V) spectra showing zero bias Kondo resonances measured at the center of CoTPyP and CrTPyP molecules. The resonances are fitted with a Fano-line shape function. The featureless spectra shown in each panel are measured on the bare substrate. The upper panel also displays the d^2I/dV^2 spectrum measured on CoTPyP. The bias difference between the minimum and the maximum in the d^2I/dV^2 spectrum around zero bias defines the full width of the resonance. The set points for spectroscopy are as follows: 50 mV, 0.2 nA, and 1 mV lock-in amplitude for the top panel spectra and 300 mV and 2 nA, and 1 mV lock-in amplitude for the bottom panel spectra.

0.6 Å increase upon atom insertion, an effect that was also observed for porphyrins doped with Fe, Co or Cr atoms.[6,9]

The effect that magnetic atom deposition has on the self-assembled TPyP molecules depends on their packing density. For instance, the Co/Cr atomic depositions onto the close-packed monolayer structures preserve the self-organization of the molecules, whereas the TPyP porous monolayer structures are destroyed by addition of Co/Cr atoms (see Fig. S2 from ESI† for more details). The close-packed structures that prevail are mostly square-lattice arrangements like those shown for CoTPyP and for CrTPyP in Fig. 1(a) and (b) but not always (see pattern B in Fig. 1(a)). Pattern A displays a square lattice with nearest neighbour separation of 1.4 nm; in this case the pyridyl groups are engaged in four-fold bonds (see Fig. S1 in ESI† for a schematic illustration of the network structures). The second pattern, pattern B, consists of alternating rows of molecules, with molecules in two adjacent rows having different orientation. Pattern B has an oblique unit cell formed by a mixture of 2- and 3-fold interacting pyridyls as seen in the schematic drawing presented in Fig. S1 of ESI.†

Measurements of the local density of states (LDOS) around the Fermi level performed at 4.5 K reveal the magnetic properties of CoTPyP and CrTPyP molecules and confirm the metalation of the porphyrin macrocycle by the magnetic centers. Fig. 2 displays high-resolution d*I*/d*V* spectra measured on the CoTPyP, CrTPyP, and on the bare substrate as well as the d^2I/dV^2 spectrum measured at the center of CoTPyP. A very pronounced zero bias peak (ZBP) is detected at the center of both molecules and is interpreted as a Kondo resonance.[25,26] The asymmetric shape of the CoTPyP ZBP may be due to a near filled state peak, which was also observed in other Kondo systems adsorbed on Au(111).[14,27] The observed Kondo resonances reflect the screened magnetic moment and advocate the magnetic nature of the molecules.[6] The corresponding Kondo temperature was determined by Fano-line fitting[28,29] of the ZBP. At 4.5 K, T_K equals 53 ± 10 K for CoTPyP and 106 ± 15 K for CrTPyP.[30] Interestingly, the d*I*/d*V* spectra of the CoTPyP molecules display additional peaks on both sides of the ZBP as illustrated in Fig. 3(a). These side peaks repeat every 80 mV and are accompanied by two step-like

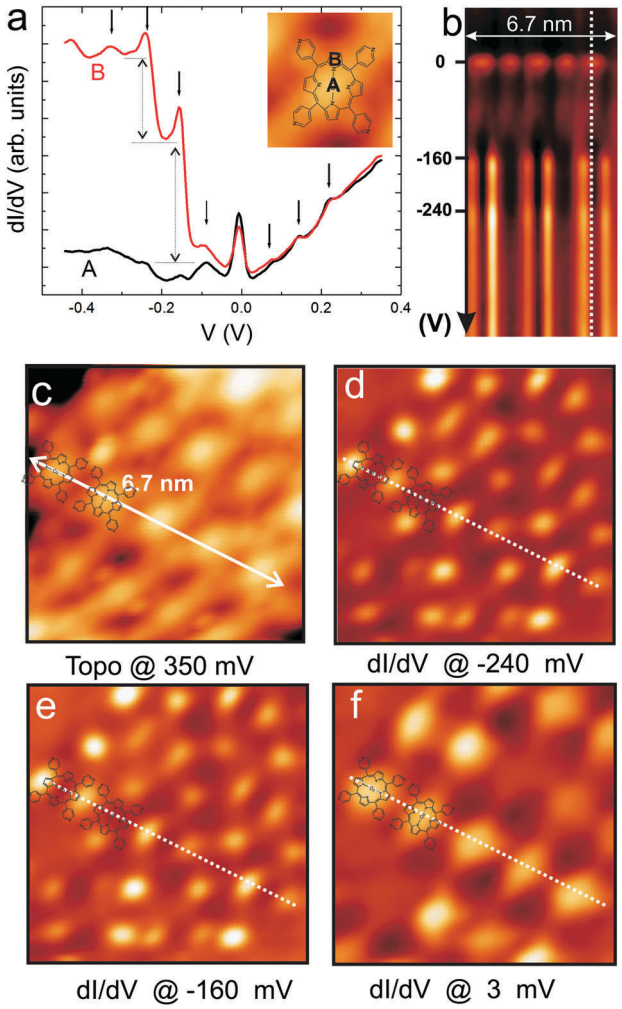

Fig. 3 (a) d*I*/d*V* spectra measured on CoTPyP molecules at the locations marked in the inset by A and B. The 80 mV-spaced Kondo replicas are marked by arrows on top of the spectra. The jumps in the d*I*/d*V* spectra marked at −160 mV and −240 mV are due to inelastic tunneling *via* vibrational levels. The relative intensity of these features depends on the location and reflects resonant tunneling. (b) A 2D representation of the d*I*/d*V* signals as a function of bias (0.1 V to −0.5 V) and distance. The spectra are measured along the double sided arrow marked in panels (c). The dotted line is added as guidance to highlight the mutually exclusive areas that contribute to the ZBP and vibrational modes. (c) STM topography (0.35 V, 340 pA) and (d)–(f) d*I*/d*V* maps of close-packed CoTPyP molecules. The voltage bias for each image is stated below each panel. The d*I*/d*V* maps were recorded with a tip height corresponding to 0.35 V and 340 pA.

increases at biases of −160 and −240 mV, respectively. The step-like increases in d*I*/d*V* spectra are well-known signatures of molecular vibrations.[31] We assign the side peaks observed in CoTPyP to Kondo resonance replicas based on previous studies that show that electronic transport through vibrating molecules can lead to emergence of peaks in the conductance[18,32] or to the appearance of Kondo replica at energies (biases) that match multiples of phonons frequencies (see Fig. S3 in ESI† for an illustration of the tunneling processes involved and and see Fig. S4 for d*I*/d*V* spectra in a broader voltage range revealing more replicas).[22,33] Kondo resonance replicas, also referred to as vibrational Kondo resonances, have been observed for organic charge–transfer complexes[34] at single phonon energy and have not yet been observed for porphyrin-based molecules. In CoTPyP, the ZBP and the 80 mV-spaced peaks are observed on the entire porphyrin macrocycle (see Fig. 3(a)). The spatial extent of the magnetic and vibrational features of the molecules are best visualized in d*I*/d*V* maps (see Fig. 3(b) and (d)–(f)), which help explain their origin. The ZBP signal is dominant across the whole porphyrin macrocycle, which suggests hybridization between the metal center and the ligand (Fig. 3(f)). The −160 and −240 mV vibrational features emerge at the periphery of the macrocycle, more exactly near two opposite pyrrole groups (see Fig. 3(d) and (e)). By comparison with available experimental data and theoretical calculation of vibrational modes in similar molecules[8,35–37] (see Table S1 of ESI†) we may assign the 160 mV molecular vibrations to stretching of C–N and C–C bonds around the pyrrole units in the macrocycle, which is in agreement with the determined spatial distribution for the 160 mV feature. According to the conductance map presented in Fig. 3(e), the 240 mV vibrations appears to share the same origin as the 160 mV vibrations. However, the 80 mV-spaced Kondo replicas are a consequence of electron coupling to an 80 mV phonon. Lower energy vibrations are considered to be resulting from metal–ligand vibrations often mixed with porphyrin deformations.[37–39]

The presence of the electron–phonon coupling inside the molecule may also explain the lower T_K measured for the *in situ* synthesized CoTPyP molecules. In general, the T_K of Co-porphyrin derivates ranges between 100 K and 550 K[10,11,20,40,41] as a function of the supporting substrate and of the functionalization of the porphyrin macrocycle. In particular, on a Au(111) substrate, CoTPP yield a T_K around 225 K[41] whereas chemically synthesized (*ex situ*) CoTPyP yield a T_K in the range of 100–118 K when they are part of a molecular array. A recent theoretical investigation by Roura-Bas *et al.*[22] of nonequilibrium transport through magnetic vibrating molecules led to the conclusion that the Kondo temperature will vary in the presence of electron–phonon coupling: a decrease in the T_K is expected with increasing electron–phonon coupling due to renormalization of the hybridization.[22] The lower T_K measured for the *in situ* synthesized CoTPyP molecules plus the additional Kondo replicas present on both sides of the Fermi level suggest the presence of stronger electron–phonon interactions in this system than in the other molecular systems mentioned. The absence of electron–phonon coupling in CrTPyP molecules may be due to stronger molecule–substrate interactions that quenches the electron–phonon coupling and enhances the spin–electron coupling as observed previously for CrTPyP on Ag(111) surface.[6] Use of complementary techniques like X-ray absorption spectroscopy and X-ray magnetic circular dichroism based measurements may reveal additional information on the magnetism of CoTPyP and CrTPyP and on their interaction with the underlying substrate. Moreover, future theoretical studies of such systems may not only help to further understand their properties but may also suggest new ways to experimentally tailor the magnetic properties of molecules by controlling the electron–phonon interactions.

Finally, we want to discuss the effect of the deposited adatom coverage on the molecular networks. The outcome of

the magnetic-atom deposition onto the TPyP close-packed molecular structures is two fold and can be summarized as follows. On one hand, adatom coverages below one per molecule mostly lead to the creation of magnetic molecules as discussed in detail above. On the other hand, adatom coverages exceeding one adatom per molecule provide excess magnetic adatoms to decorate the molecular assembly at the hollow sites (intermolecular junctions) forming organo-metallic networks. Interestingly, the formation of such lattices is observed only for molecular patterns of type A indicating a preferential four-fold binding of Co (Cr) to pyridyl ligands. Careful inspection of high-resolution STM images like those presented in Fig. 1 can help discriminate between different occupation of the molecular junctions: single atom inserted at the four-pyridyl junction (marked by an arrow) can be easily distinguished from the empty junction or from the multi-atom features (marked by a dotted circle).[21] Beside visual inspections of the structural properties, conductance measurements are also necessary to characterize these single- or multi-atom junctions.[42] A description of the magnetic properties of these metallic junctions is presented in Section III of ESI.†

In conclusion, we probed electron–phonon interactions in synthesized magnetic metalloporphyrins using scanning tunneling spectroscopy and Kondo physics. The magnetic molecules were synthesized *in situ via* chemical reactions between TPyP molecules and magnetic atoms (Co and Cr). Our results show that both synthesized molecules develop a magnetic moment upon doping and their surface assemblies can be used as potential templates for realization of organometallic networks or periodic arrangement of metallic particles. However, electron–phonon interactions that lead to interplay between Kondo physics and vibrational excitations are observed only in CoTPyP molecules. Exploiting electron–phonon interactions in metallo-organic molecules may open up novel routes for tailoring their magnetic properties for use in molecular spintronics.

This work has been supported by the Research Foundation – Flanders (FWO, Belgium). Z. L. acknowledges the support from the China Scholarship Council (No. 2011624021) and from Internal KU Leuven funds.

References

1 S. Sanvito, *Chem. Soc. Rev.*, 2011, **40**, 3336–3355.
2 W. Auwärter, D. Ecija, F. Klappenberger and J. V. Barth, *Nat. Chem.*, 2015, **7**, 105.
3 W. Auwärter, A. Weber-Bargioni, A. Riemann, A. Schiffrin, O. Gröning, R. Fasel and J. V. Barth, *J. Chem. Phys.*, 2006, **124**, 194708.
4 F. Klappenberger, A. Weber-Bargioni, W. Auwärter, M. Marschall, A. Schiffrin and J. V. Barth, *J. Chem. Phys.*, 2008, **129**, 214702.
5 Z. Shi and N. Lin, *J. Am. Chem. Soc.*, 2009, **131**, 5376–5377.
6 K. Schouteden, Ts. Ivanova, Z. Li, V. Iancu, E. Janssens and C. Van Haesendonck, *J. Phys. Chem. Lett.*, 2015, **6**, 1048–1052.
7 Y. Li and N. Lin, *Phys. Rev. B*, 2011, **84**, 125418.
8 H. Kim, Y. H. Chang, S.-H. Lee, S. Lim, S.-K. Noh, Y.-H. Kim and S.-J. Kahng, *Chem. Sci.*, 2014, **5**, 2224–2229.
9 W. Auwärter, A. Weber-Bargioni, S. Brink, A. Riemann, A. Schiffrin, M. Ruben and J. V. Barth, *ChemPhysChem*, 2007, **8**, 250–254.
10 A. Zhao, Q. Li, L. Chen, H. Xiang, W. Wang, S. Pan, B. Wang, X. Xiao, J. Yang, J. G. Hou and Q. Zhu, *Science*, 2005, **309**, 1542–1544.
11 V. Iancu, A. Deshpande and S.-W. Hla, *Nano Lett.*, 2006, **6**, 820–823.
12 A. Mugarza, C. Krull, R. Robles, S. Stepanow, G. Ceballos and P. Gambardella, *Nat. Commun.*, 2011, **2**, 490.
13 G. D. Scott and D. Natelson, *ACS Nano*, 2010, **4**, 3560–3579.
14 T. Komeda, H. Isshiki, J. Liu, Y.-F. Zhang, N. Lorente, K. Katoh, B. K. Breedlove and M. Yamashita, *Nat. Commun.*, 2011, **2**, 217.
15 J. Chen, M. A. Reed, A. M. Rawlett and J. M. Tour, *Science*, 1999, **286**, 1550–1552.
16 N. P. Guisinger, M. E. Greene, R. Basu, A. S. Baluch and M. C. Hersam, *Nano Lett.*, 2004, **4**, 55–59.
17 R. P. Andres, T. Bein, M. Dorogi, S. Feng, J. I. Henderson, C. P. Kubiak, W. Mahoney, R. G. Osifchin and R. Reifenberger, *Science*, 1996, **272**, 1323–1325.
18 A. Riss, S. Wickenburg, L. Z. Tan, H.-Z. Tsai, Y. Kim, J. Lu, A. J. Bradley, M. M. Ugeda, K. L. Meaker, K. Watanabe, T. Taniguchi, A. Zettl, F. R. Fischer, S. G. Louie and M. F. Crommie, *ACS Nano*, 2014, **8**, 5395–5401.
19 V. Iancu, K.-F. Braun, K. Schouteden and C. Van Haesendonck, *Phys. Rev. Lett.*, 2014, **113**, 106102.
20 Q. Zhang, G. Kuang, R. Pang, X. Shi and N. Lin, *ACS Nano*, 2015, **9**, 12521–12528.
21 T. Lin, G. Kuang, W. Wang and N. Lin, *ACS Nano*, 2014, **8**, 8310–8316.
22 P. Roura-Bas, L. Tosi and A. A. Aligia, *Phys. Rev. B*, 2013, **87**, 195136.
23 All experiments are conducted in a UHV system (base pressure of 10–11 mbar) that includes an Omicron low temperature STM operated at 4.5 K.
24 A detailed analysis on the dehydrogenation of TPyP macrocycle triggered by insertion of Co and Cr is given in ref. 6.
25 V. Madhavan, W. Chen, T. Jamneala, M. F. Crommie and N. S. Wingreen, *Science*, 1998, **280**, 567–569.
26 J. Li, W.-D. Schneider, R. Berndt and B. Delley, *Phys. Rev. Lett.*, 1998, **80**, 2893–2896.
27 J. Liu, H. Isshiki, K. Katoh, T. Morita, B. K. Breedlove, M. Yamashita and T. Komeda, *J. Am. Chem. Soc.*, 2013, **135**, 651.
28 U. Fano, *Phys. Rev.*, 1961, **124**, 1866–1878.
29 O. Újsághy, J. Kroha, L. Szunyogh and A. Zawadowski, *Phys. Rev. Lett.*, 2000, **85**, 2557–2560.
30 These measurements are carried out only on molecules that are part of a square molecular network and therefore we do not comment on the effect that the network has on their magnetic properties as was presented recently in ref. 20 and 21.
31 B. C. Stipe, M. A. Rezaei and W. Ho, *Science*, 1998, **280**, 1732–1735.
32 N. B. Zhitenev, H. Meng and Z. Bao, *Phys. Rev. Lett.*, 2002, **88**, 226801.
33 Z.-Z. Chen, H. Lu, R. Lu and B. Zhu, *J. Phys.: Condens. Matter*, 2006, **18**, 5435–5446.
34 I. Fernández-Torrente, K. J. Franke and J. I. Pascual, *Phys. Rev. Lett.*, 2008, **101**, 217203.
35 A. Atamian, R. J. Donohoe, J. S. Lindsey and D. F. Bocian, *J. Phys. Chem.*, 1989, **93**, 2236–2243.
36 Z. Zhang, S. Hou, Z. Zhu and Z. Liu, *Langmuir*, 2000, **16**, 537–540.
37 K. F. Domke and B. Pettinger, *ChemPhysChem*, 2009, **10**, 1794.
38 D. Li, Z. Peng, L. Deng, Y. Shen and Y. Zhou, *Vib. Spectrosc.*, 2005, **39**, 191–199.
39 J. Kincaid and K. Nakamoto, *J. Inorg. Nucl. Chem.*, 1975, **37**, 85–89.
40 A. Zhao, Z. Hu, B. Wang, X. Xiao, J. Yang and J. G. Hou, *J. Chem. Phys.*, 2008, **128**, 234705.
41 H. Kim, Y. H. Chang, S.-H. Lee, Y.-H. Kim and S.-J. Kahng, *ACS Nano*, 2013, **7**, 9312–9317.
42 T. Jamneala, V. Madhavan and M. F. Crommie, *Phys. Rev. Lett.*, 2001, **87**, 256804.

